

First Results from a Retarding Field Angle-Resolved Analyzer

W. J. Antel Jr., G. R. Harp
Department of Physics and Astronomy
Ohio University
Athens, OH 45701
USA

A LEED-like display analyzer is discussed. It uses four retarding field grids and projects the electron distribution onto a hemispherical phosphor screen. However, this analyzer has no coaxial electron gun, which permits measurements of electron intensity over a large angular range. A fiber-optic faceplate projects the hemispherical image onto a plane, where the light intensity is measured ex-situ with a high dynamic range CCD camera. This analyzer is optimized for angle-resolved Auger and photoemission spectroscopy. We evaluate the effectiveness of this analyzer for the measurement of angle-resolved diffraction patterns for use in electron holography.

I. Introduction

In the field of surface science, the techniques of low energy electron diffraction (LEED) [1], Auger electron diffraction (AED), and x-ray photoelectron diffraction (XPD) [2] are often used for structure determination. All three techniques rely upon analysis of the angular distribution of electrons diffracted from a sample of interest. The type of detector used is determined by two factors: 1) the number, and 2) the energy of electrons in the angular distribution. A hemispherical analyzer is the mainstay for AED and XPD, due to both methods low electron yield [3]. This type of analyzer has the advantage of high sensitivity, but the disadvantage of long data collection times and high cost. LEED, which has a large electron yield, uses a less sensitive angle-resolved display analyzer [1]. Here the electrons are imaged as they strike a hemispherical phosphor coated screen. An advantage to this type of detector is that data acquisition times are short, however, traditional LEED analyzers have the electron gun situated coaxial with the screen. Thus it is impossible to collect data from the central 10° of the analyzer. In using a LEED detector for AED/XPD, the loss of data from the central region poses a greater problem. The entire diffraction pattern is required for these techniques, especially if one is using them for electron holography [4]. Another reason that hemispherical analyzers have been used for AED/XPD is their low electron yield. LEED detectors are not sensitive enough to image the diffraction pattern. More specifically, methods used for imaging the LEED screen lacked sensitivity. We argue that with the advent of charge coupled device (CCD) cameras, this is no longer the case and AED/XPD patterns can be recorded. Thus there was a motivation to develop a LEED-like analyzer without a coaxial electron gun. The realization of this development is discussed in the following sections.

II. Vacuum System Design

The design of the chamber was dictated by several key factors. The first was being able to transfer a thin film sample in situ from the attached magnetron sputtering growth chamber. Second, was the need that both an Auger electron gun and laboratory X-ray source coexist without interfering in the operation of one another. The result is that the electron gun, X-ray anode, and detector are mounted so as to lie in a single plane. The sample to be studied is then positioned in this plane using a five axis goniometer.

The analysis chamber is right cylindrical, 0.61m in diameter and long, mounted on its side. It is pumped with an ion pump. On one end, is a 1m linear transfer arm with an attached carriage. This is used to move a sample from the sputter growth chamber into the analysis chamber. The sample is then transferred to the goniometer. This is a EM200 Series manipulator manufactured by Thermionics Northwest, Inc. of Port Townsend, WA. Its five axes of motion are θ and ϕ rotations, and x , y , and z translations. The two rotation axes can be computer controlled with stepper motors. The sample stage itself can be cooled using liquid nitrogen. The z-axis (horizontal) motion can move the sample to the opposite end of the chamber where the x-ray anode, electron gun, and analyzer are located. A schematic of this end of the chamber is shown in figure 1.

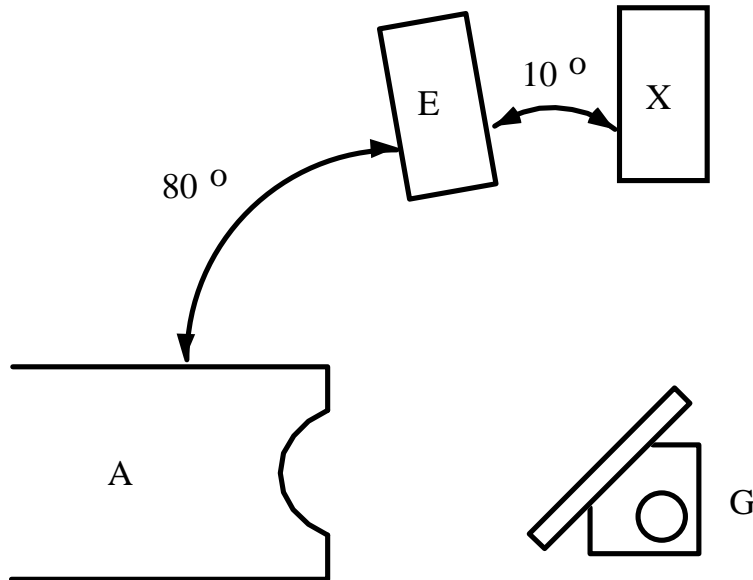


Figure 1. Layout of analysis end of chamber. The electron gun (E), the analyzer (A), and the x-ray anode (X) all lie in the same plane. Their angles with respect to one another are shown. The goniometer (G), is used to move the sample into this plane. Its two rotation axes are then used to change the sample's angle.

The Auger electron gun is mounted on a port aligner at an angle of 80° to the detector. There is a distance of approximately 0.15m between the gun and the sample. This gun is manufactured by Kimball Physics of Wilton, NH. It is capable of emission energies over a wide range from 300eV to 5keV. Emission current, which is regulated by a feedback circuit, has a maximum value of 0.5mA. The beam spot size is approximately 2mm.

The X-ray source is mounted next to the electron gun, at an angle of 90° to the detector. This source has a Mg anode, capable of being run at 800W. It is manufactured by VG Microtech of East Sussex, UK. When in use, the anode is positioned within 0.05m of the sample. A collimator limits the beam spot size to approximately 0.01m.

As was mentioned in the introduction, part of the motivation for constructing a system of this type was the advent of sensitive CCD cameras. A Photometrics CH250 camera head is used in this system. This particular model has a Thomson TH7896 1024x1024 CCD chip. The associated electronics are capable of digitizing images to a depth of 12 bits. The camera, as well as other data acquisition described below, is controlled via a PC running National Instruments' LabVIEW. The virtual instruments (software programs) were written in house.

III. Retarding Field Angle-resolved Analyzer

A schematic of the detector appears in figure 2. It is manufactured by OCI Vacuum Microengineering of London, Ontario based on our designs. The detector, which has a 100° angle of acceptance, is mounted on a standard double-sided 8" flange (labeled F in the figure). One side mounts to the chamber, while the other mounts an 8" glass viewport with an antireflective coating (labeled W in the figure). The screen/grid assembly is mounted on an in-situ linear motion stage. This allows the detector to be retracted out of harms way during sample transfer.

Energy selection is performed by four grids, these are labeled 1-4 in the schematic. Each is a tungsten wire mesh that has been carbon and gold coated. Grid 1 is held at ground potential. There is also a solid cylindrical ground shield enclosing the whole grid assembly. Both of these serve to isolate the rest of the chamber from stray fields. Each of grids 2 through 4 can be tuned to an independent potential, up to 3keV. In the current configuration, however, grids 2 and 3 are tied together. As can be seen in the schematic, these two grids are relatively close together compared to the other grid spacings. When a negative voltage is applied, a region of uniform potential is formed between them. This provides a uniform retarding field for the analyzer. Grid 4 is tied to chamber ground in the current configuration.

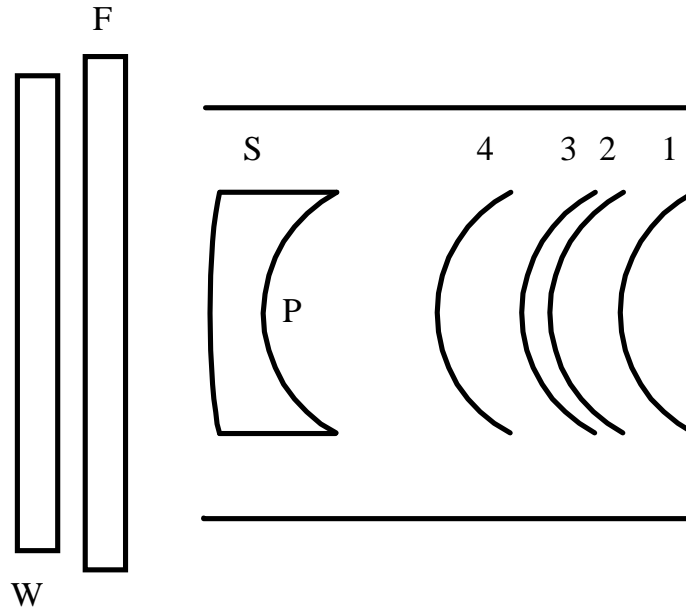


Figure 2. Schematic of angle-resolved retarding field analyzer. (W) 8" glass viewport, (F) Double-sided vacuum flange, (S) Fiber-optic screen, (1-4) Gold coated Tungsten hemispherical meshes. (P) denotes the side of the screen that is coated with phosphor.

Why are grids 2 through 4 wired independently? A small percentage of the electrons passing through the grids, will strike the wire mesh. When this happens, a number of low energy electrons are emitted. These secondary electrons will be detected at the screen as noise. It should be clear that the probability of an electron striking the grid is highest at the grid closest to the sample, namely grid 2. One way to reduce this noise is to tune each grid independently. An example illustrates this best. Say one wants a retarding field of 1kV, then grids 2, 3, and 4 should be set to negative potentials of 990V, 1kV, and 500V respectively. With these settings, the majority of secondary electrons (those from grid 2), are blocked from getting through to the screen by the higher potential on grid 3. Likewise, the electrons are not too strongly accelerated between grids 3 and 4, limiting the number of secondaries generated at grid 4.

The diffraction pattern is imaged on a phosphor and aluminum coated fiber-optic screen (labeled S in the figure). It is disk shaped, with a radius of 0.061m. The purpose of the fiber-optic is to map the spherical diffraction pattern to a plane thus reducing the aberrations in the image (most camera optics are optimized to focus in a plane,). The side of the screen facing the grids is hemispherical with a curvature radius of 0.075m. This face is coated with P-20 phosphor which emits light at a peak wavelength of 540nm. On top of the phosphor is a thin film of aluminum that provides a

conducting layer. During operation, a positive potential of 5kV is applied to the screen. This accelerates the electrons into the phosphor, causing it to emit light. The side of the screen opposite the grids has a slight convex curvature (radius=-0.254m). Fiber-optic is optimized for normal emission. Thus, without this curvature, the CCD camera would be less sensitive to the region around the edge of the screen.

The high voltage (HV) potentials for the grids and screen are supplied with standard modular HV supplies. These were assembled in house into a single unit. During operation, the potential on the grids and screen can be set either manually or through computer control.

IV. Techniques: LEED, XPD, AED, AES, and XPS

As was previously mentioned, the analyzer can be used for LEED, XPD and AED. It is also possible to obtain Auger spectra (AES) [5], X-ray photoemission spectra (XPS) [6], and Kikuchi electron diffraction (KED, quasi-elastic electron diffraction). Operation of the detector for each of these techniques is outlined below. KED is presented with results in section V.

Auger spectroscopy is performed by using the analyzer as an angle integrating detector. The signal is measured using lock-in methods. In its simplest realization, grids 1 and 4 are grounded to the chamber. Grids 2 and 3 are tied together and used for energy selection. The modulation required for the use of a lock-in amplifier is coupled on top of the HV of grids 2 and 3 with the aid of a transformer. This can be seen in the schematic in figure 3. The transformer used is optimized for high frequency (i.e. it has a low loss), and has a dielectric rated up to 3.7kV. A bias voltage (V in the figure) of +270V is applied to the screen using batteries. A lock-in amplifier (L), which is coupled to the batteries through a high impedance transformer, is used to measure the electron current to ground. Control of the experiment is through a PC running National Instruments' LabVIEW, with their LabPC+ data acquisition board. XPS is done with the analyzer in the same configuration.

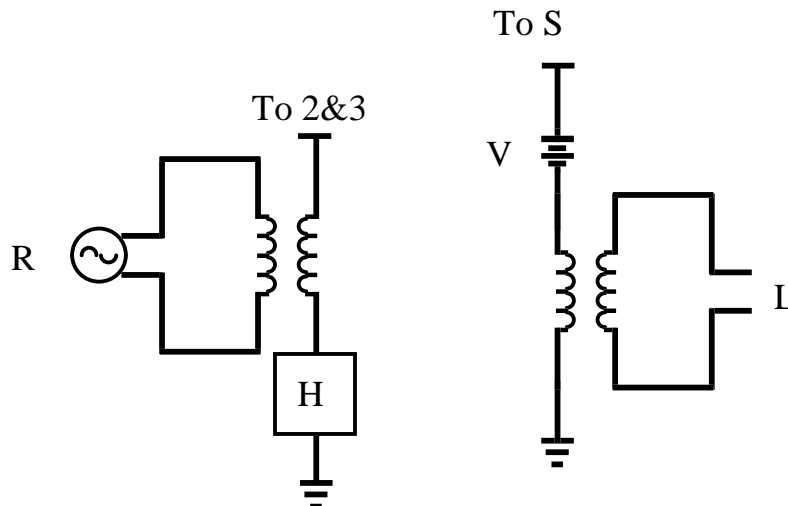


Figure 3. Wiring diagram for performing AES with this analyzer. (R) is reference signal from lock-in detector, this is coupled on top of the high voltage (H) of grids 2 and 3 using a signal transformer. (L) is connected the input of the lock-in detector. This input is coupled to the screen with a transformer. The screen is biased with a battery (V).

When performing XPD/AED, one is interested in the angular distribution of electrons that are associated with a certain transition. Although each of these transitions occur at a fixed point, there is an energy spread associated with each. This spread corresponds to the peak width in the energy spectrum. In order to obtain a pattern from all of the electrons in one transition, it is thus necessary to integrate over the entire peak. A differencing scheme is employed to do this. The detector is configured as was described above in section III. An angle-resolved pattern is digitized for two separate energies that define the energy spread of the transition. The difference of these two images leaves an angle-resolved diffraction pattern for that one transition.

Another surface analysis technique that can be done with this detector is LEED. The electron gun in the system is optimized for Auger spectroscopy: its energy range bottoms out at 300eV. Generally LEED is performed with electrons of a lower primary energy. This aside, it is still possible to perform LEED on this system. The screen is biased at 5kV, and grids 2 and 3 are tuned manually to just below the primary electron energy. As a result, only those electrons that are elastically scattered from the crystal are imaged. These diffraction patterns are then digitized with the CCD camera.

V. Technique: KED

A Kikuchi diffraction pattern of a Pt (100) surface is shown in figure 4. These images are useful in that much of the same information that is present in an XPD image can also be extracted from a Kikuchi pattern [7]. In LEED, electrons scatter elastically from the atoms in the crystal. As a result, the scattering is coherent, and the outgoing scattered electrons interfere with one another constructively in the Bragg directions. In all other directions the interference is destructive. As the energy of the incoming electron is increased, its wavelength decreases, hence it becomes more sensitive to the quasi-static distortion of the crystal lattice caused by phonons. A scattering event of this type has a small energy loss, thus it can be considered to be quasi-elastic. However, the outgoing electron waves are no longer coherent with one another. The result is the diffuse scattering pattern seen in the figure.

Figure 4. Kikuchi diffraction pattern for a Pt (100) surface. The electron beam energy is 2.8kV .
(a) Original image digitized directly from the screen; (b) Image to which processing steps (described in text) have been applied.

The Pt film was deposited on an MgO (100) oriented substrate using the attached magnetron sputtering system. This system has a base pressure of 1×10^{-9} Torr, and a 3.25mTorr Ar atmosphere during sputtering. Before growth the substrate was polished with an 0.05μ alumina solution, and then annealed at 600° C. Epitaxy was obtained through the use of established methods [8]. A buffer layer of 4\AA Fe and 25\AA Pt layer were deposited at 600° C. On top of this was grown 320\AA of Pt at a temperature of 300° C .

A KED pattern was obtained using a 2.8kV electron energy, and the detector grids tuned as for LEED. To this pattern, image processing was performed (see below). The original image and the processed result are shown in figure 4. The four-fold symmetry of the (100) orientation is readily apparent. A couple of the many crystal directions that can be seen: 1) the central spot is the (100) direction, and 2) the brightest spots at the four corners of a horizontal square are from scattering along the (101) direction.

Finally, a brief note should be made about the processing done to the original digitized image. This is felt to be relevant due to the small number of steps involved. First, the image was enhanced using a standard technique called flat fielding [9]. Before going on to the second step, note the original image forms one fourth of that shown in the figure. To apply the four-fold symmetry, the original image had to be rotated so that the (100) spot was in one corner. This rotation operation is simplified due to the fiber-optic screen mapping the spherical diffraction pattern into a plane. The final step was to rotate, in the image plane, three copies of the original to fill in the remaining three quadrants.

VI. Conclusion

The applicability of this detector to multiple analysis techniques makes it a versatile addition to the lab. It features a fiber-optic screen, which aids in the digitizing of angle-resolved diffraction patterns. Energy selection is performed with four hemispherical grids that can all be independently tuned. Promising results have been obtained using the analyzer as an integrating detector while taking Auger and XPS spectra (not shown). Additionally, when used as an angle-resolved analyzer, the detector shows promise for XPD/AED. A KED pattern from a Pt (100) surface has also been presented.

VII. Acknowledgments

The authors gratefully acknowledge support of the Ballistic Missile Defense Organization AASERT Grant No. N0014-97-0742 and URISP Grant No. N00014-96-1-0782 under the auspices of the Office of Naval Research with grant monitors Colin Wood and Jürgen Pohlmann.

1. M.A. Van Hove, W.H. Weinberg, C.M. Chan, Low Energy Electron Diffraction: Experiment, Theory, and Surface Structure Determination, Springer-Verlag, New York (1986). pp. 20-21.
2. C.S. Fadley, in Synchrotron Radiation Research: Advances in Surface Science, R.Z. Bachrach, ed., Plenum Press, New York, (1990).
3. M. Prutton, Introduction to Surface Physics, Oxford University Press, New York (1994). pp. 17.
4. John J. Barton, Photoelectron Holography, Phys. Rev. Lett. 61:1356-1359 (1988).
5. C.R. Brundle and A.D. Backer, Electron Spectroscopy: Theory, Techniques, and applications, Academic Press, London (1981).
6. P. Weightman, Rep. Prog. Phys. 45:753 (1982).
7. S.A. Chambers, I.M. Vitomirov, S.B. Anderson, J.H. Weaver, Medium-energy Backscattered Electron Diffraction as a Probe of Elastic Strain in Epitaxial Layers, Phys. Rev. B, 35:2490 (1987).
8. G. R. Harp, S. S. P. Parkin, Seeded Epitaxy of Metals by Sputter Deposition, Appl. Phys. Lett. 65:3063 (1994).
9. Photometrics, Ltd., Charge-Coupled Devices for Quantitative Electronic Imaging, Photometrics, Ltd., Tucson, AZ (1992). pp. 34-35.